Dissolved organic nitrogen in the global surface ocean: Distribution and fate

Robert T. Letscher,[1,2] Dennis A. Hansell,[1] Craig A. Carlson,[3] Rick Lumpkin,[4] and Angela N. Knapp[1]

Received 16 July 2012; revised 13 November 2012; accepted 27 November 2012; published 26 February 2013.

[1] The allochthonous supply of dissolved organic nitrogen (DON) from gyre margins into the interior of the ocean's oligotrophic subtropical gyres potentially provides an important source of new N to gyre surface waters, thus sustaining export production. This process requires that a fraction of the transported DON be available to euphotic zone photoautotroph communities via mineralization. In this study, we investigated the biological and physical controls on the distribution and fate of DON within global ocean surface waters. Inputs of nitrate to the euphotic zone at upwelling zones fuel net accumulation of a DON pool that appears to resist rapid microbial remineralization, allowing subsequent advective transport into the subtropical gyres. Zonal gradients in DON concentrations across these gyres imply a DON sink in the surface layer. Assessment of the physical dynamics of gyre circulation and winter mixing revealed a pathway for DON removal from the mixed layer via vertical transport to the deep euphotic zone, which establishes the observed zonal gradients. Incubation experiments from the Florida Straits indicated surface-accumulated DON was largely resistant (over a few months) to utilization by the extant surface bacterioplankton community. In contrast, this same material was remineralized three times more rapidly when exposed to upper mesopelagic bacterioplankton. These results suggest the primary fate of surface DON to be removal via vertical mixing and subsequent mineralization below the mixed layer, implying a limited role for direct DON support of gyre export production from the surface layer. DON may contribute to export production at the eastern edges of the subtropical gyres, but only after its mineralization within the deep euphotic zone.

Citation: Letscher, R. T., D. A. Hansell, C. A. Carlson, R. Lumpkin, and A. N. Knapp (2013), Dissolved organic nitrogen in the global surface ocean: Distribution and fate, *Global Biogeochem. Cycles*, *27*, 141–153, doi:10.1029/2012GB004449.

1. Introduction

[2] Over much of the surface global ocean (upper 200 m), most of the standing stock of fixed nitrogen (N) is in the form of dissolved organic nitrogen (DON) [*Bronk*, 2002; *Aluwihare and Meador*, 2008]. Accumulation of N within this pool results from a decoupling of DON production and consumption processes primarily carried out by autotrophic plankton and heterotrophic bacterioplankton, respectively. This biologically recalcitrant material can accumulate via direct production [*McCarthy et al.*, 2004] or diagenetic alteration of the molecular structure [*Amon and Benner*, 1996]. However, if a portion of the euphotic zone (<100 m) bulk DON pool eventually becomes bioavailable to the resident microbial community, then the remineralized N can represent a potential source of new N to support primary and export production in oligotrophic systems.

[3] Prior efforts to quantify the sustenance of upper ocean productivity by DON have focused on the Atlantic Ocean where the greatest density of DON observations exists and a clear east-to-west gradient in DON concentration has been observed (>5 μmol kg^{-1} in the east to ~4.5 μmol kg^{-1} in the west) [*Mahaffey et al.*, 2004; *Roussenov et al.*, 2006; *Charria et al.*, 2008; *Torres-Valdés et al.*, 2009]. These studies have considered the allochthonous input of semilabile DON (lifetime of months to years), generated at the productive gyre margins, to the subtropical gyre interior and its potential role as an organic nutrient for enhancing export production there. In order for allochthonous DON to be a quantitatively important source of new N, a substantial fraction of the advected DON must become bioavailable to the photoautotrophic community within the euphotic zone. Mechanisms that make DON bioavailable to photoautotrophs include direct assimilation [*Bronk et al.*, 2007], extracellular

[1]Rosenstiel School of Marine and Atmospheric Science, University of Miami, Miami, Florida, USA.
[2]Now at Earth System Science, University of California, Irvine, California, USA.
[3]Ecology, Evolution, and Marine Biology, University of California, Santa Barbara, California, USA.
[4]Atlantic Oceanographic and Meteorological Laboratory, NOAA, Miami, Florida, USA.

Corresponding author: Robert T. Letscher, Earth System Science, University of California, Irvine, California, USA. (robert.letscher@uci.edu)

0886-6236/13/2012GB004449

hydrolysis [*Palenik and Morel*, 1991], heterotrophic remineralization to inorganic N with subsequent uptake [*Bronk*, 2002], and photo-oxidation to NH_4^+ [*Bushaw et al*., 1996]. Considering these euphotic zone sinks for DON, the annual advective flux of bioavailable DON to the North Atlantic subtropical gyre ranges from ~0.01 to 0.08 mol N m^{-2} yr^{-1} [*Mahaffey et al*., 2004; *Roussenov et al*., 2006; *Charria et al*., 2008; *Torres-Valdés et al*., 2009], similar in magnitude to rates of advective supply of inorganic nutrients [i.e., nitrate (NO_3^-)] [*Williams and Follows*, 1998] and N_2-fixation [*Gruber and Sarmiento*, 1997; *Hansell et al*., 2004]. If these rates are accurate, the process supplies a significant amount of the N needed to explain geochemical estimates of export production in that system [*Jenkins and Wallace*, 1992].

[4] An alternative fate for surface ocean DON is vertical transport (by mixing and/or subduction, hereafter referred to as overturning circulation) to depth (>100 m), with subsequent mineralization by mesopelagic heterotrophic bacterioplankton. *Abell et al*. [2000] reported that DON remineralization along subsurface isopycnals, initially ventilated by subduction, explained ~20% of oxygen demand in the upper mesopelagic (100 to 300 m). In a study of the biological controls on dissolved organic carbon (DOC) utilization at the Bermuda Atlantic Time-series Study (BATS) site, *Carlson et al*. [2004] found that the surface accumulated, semilabile DOC pool was recalcitrant to the surface bacterioplankton community, but available to the bacterioplankton community within the upper mesopelagic zone (~250 m depth). Other studies at the BATS site have found euphotic zone DON to be recalcitrant to microbial utilization throughout the year [*Hansell and Carlson*, 2001; *Knapp et al*., 2005], suggesting that DON mineralization is largely restricted to the mesopelagic zone.

[5] The upper layer (<200 m) of the eastern sectors of subtropical gyres is highly modified by vertical mixing en route to the gyre interior, being sites of subtropical mode water formation [*Siedler et al*., 1987; *Hautala and Roemmich*, 1998]. The physical dynamics of gyre circulation (including vertical mixing), coupled with preferential utilization of DON by subsurface bacterioplankton, serves as an additional mechanism for establishing the observed east–west gradients in DON. Assuming this alternative model is valid, the allochthonous DON supply would not directly contribute to export production from the euphotic zone. Thus, quantifying the importance of these DON loss pathways is relevant for understanding sources of new N supporting export production in oligotrophic gyres.

[6] In this study we present the global surface ocean distribution of DON and characterize the spatial gradients. Three mechanisms are proposed to describe DON distribution and its sinks: (1) Net DON production in highly productive upwelling systems, (2) net DON removal via mineralization in support of export production from the surface euphotic zone, and (3) DON mineralization upon overturning circulation of the water column. Here we employ seawater incubation experiments to test the relative importance of mechanisms II versus III. Insights from these experiments are combined with an assessment of the physical dynamics of subtropical gyre circulation aided by use of a statistical model of the wind-driven Ekman layer, derived from drifting buoy observations to determine the primary driver of the observed upper ocean DON gradients. We conclude with an assessment of the role of allochthonous DON supply in the biogeochemistry of oligotrophic ocean gyres.

2. Methods

2.1. Field Collected Data Sets

[7] We employed observations of DON and other hydrographic variables collected on numerous oceanographic cruises as part of the U.S. Global Ocean Carbon and Repeat Hydrography program [http://ushydro.ucsd.edu/]. Observations of DOC and DON were made on full water column CTD casts at ~60 nautical mile resolution. Sample analyses were performed by the Hansell and Carlson labs at the University of Miami and University of California, Santa Barbara, respectively. Data were downloaded from CDIAC [http://cdiac.ornl.gov/oceans/RepeatSections/]. Additional observations of DON were from World Ocean Circulation Experiment (WOCE) lines I08N in 1995, A05 in 1998, U.S. Joint Global Ocean Flux Study (JGOFS) Arabian Sea Process Cruise #2 in 1995, and the NOAA North American Carbon Program (NACP) west coast cruise from 2010. The majority of the oceanographic cruise data was collected during the local summer and autumn seasons and thus captures environmental conditions during times of stratification of the surface ocean. Spring sampling was limited to line I08N in the Indian Ocean and line P16N in the Pacific Ocean.

2.2. Incubation Experiments

[8] Incubation experiments were carried out over the course of several months in the laboratory using field-collected seawater from the Florida Straits at 27º N 79.5º W on March 10, 2011 (hereafter, Exp-March) and 27º N 79.9º W on December 7, 2011 (hereafter, Exp-Dec). The surface waters at this location are stratified year-round and annual mean sea surface chlorophyll *a* concentrations are low (<0.1 mg m^{-3}) [http://disc.sci.gsfc.nasa.gov/giovanni/] with the deep chlorophyll maximum (DCM) found at ~80 to 90 m, providing an oligotrophic environment analogous to the adjacent North Atlantic subtropical gyre. The experimental objective was to quantify the remineralization potential of the surface DON pool given exposure to distinct bacterioplankton communities (surface versus upper mesopelagic). Filtered (0.2 μm) surface (10 m) seawater was mixed with whole water (unfiltered) inocula from either of 10 m or 180 m depth (Exp-March); or 10 m and 130 m depth (Exp-Dec) to test the availability of surface DON to removal by surface versus upper mesopelagic bacterioplankton communities. The dilution culture technique closely follows that used by *Carlson et al*. [2004], which allows the bacterioplankton to be released from grazer pressure, stimulating bacterial growth and substrate utilization.

[9] Seawater was collected from Niskin bottles attached to a CTD (Conductivity, Temperature, Depth) rosette and stored in acid-cleaned 10-liter polycarbonate carboys in the dark at in situ temperatures until incubation initiation on shore (within 12 hours). Eight liters of 10 m seawater were gravity filtered through an acid-cleaned Acropak 1000 Supor membrane 0.8/0.2-μm cartridge filter into incubation carboys. The 0.2-μm filtrate was inoculated with 2 L of whole water (hereafter, inoculum), which contained the resident microbial communities found within either the euphotic or upper mesopelagic zones. For Exp-March, two 10-L carboys received the 10 m surface water inoculum (hereafter, surface-surface) and 2 carboys received an inoculum from 180 m depth (hereafter, surface-meso). During Exp-Dec, 3 carboys received a 10 m surface water inoculum (surface-surface),

whereas 3 carboys received an inoculum from 130 m depth (surface-meso). The sampling depth of the mesopelagic bacterioplankton community water targeted the top of the nitracline, where $[NO_3^-] = \sim 1\ \mu mol\ kg^{-1}$ (hereafter referred to as the nitracline) [*Cullen and Eppley*, 1981] and where organic N remineralization is known to occur [*Ward et al*., 1989]. The incubation carboys were well mixed and stored in the dark at room temperature (21 ° C), slightly above the in situ temperature for each inoculum (Exp-March = 19.5 ° C; Exp-Dec = 17 ° C). Subsamples of incubation water were collected at >10 time points over the course of 90 days (Exp-March) or 180 days (Exp-Dec) to monitor for changes in the concentration of DON as well as the products of DON remineralization, i.e., ammonium (NH_4^+) and NO_3^-.

2.3. Sample Collection and Analysis

2.3.1. Sampling

[10] Samples from the oceanographic cruises were filtered for the removal of particulate organic matter (POM) using precombusted Whatman GF/F filters (nominal pore size 0.7 μm) held in acid-cleaned polycarbonate filter holders. Filter holders were connected in line with the CTD-Niskin bottle using acid-cleaned silicon tubing. Seawater was collected into acid-cleaned and preconditioned (with seawater) 60 mL HDPE bottles and immediately frozen upright at -20 ° C. Inocula for the incubation experiments were collected unfiltered to minimize contamination and to include the resident bacterioplankton population.

2.3.2. DOC and TDN concentration

[11] DOC and total dissolved nitrogen (TDN) were analyzed by high temperature combustion (HTC) using a Shimadzu (Durham, NC) TOC-VCSH system coupled with a Shimadzu Total N analyzer [*Dickson et al*., 2007]. The N oxidation product nitric oxide (NO) is quantified by reaction with ozone and detection of the resulting chemiluminescence. Standardization was achieved using potassium nitrate for TDN and potassium hydrogen phthalate for DOC. Deep seawater and low carbon (C) reference waters as provided by the Hansell CRM Program [*Hansell*, 2005] were measured every sixth analysis to assess day-to-day and instrument-to-instrument variability. The precision for TDN analyses is ~0.5 $\mu mol\ kg^{-1}$ or a CV of 5% to 10%. The precision for DOC analyses is ~1 $\mu mol\ kg^{-1}$or a CV of 2% to 3%. TDN measurements for WOCE lines A05 + I08N and U.S. JGOFS Arabian Sea Process Cruise #2 were performed by the UV-oxidation method [*Walsh*, 1989]. Measurements of TDN along WOCE line P18 using the UV method [*Hansell and Waterhouse*, 1997] were typically ~10% higher than those from the more recent CLIVAR occupation of the line using the HTC method (both cruises were analyzed by Hansell laboratory, University of Miami).

2.3.3. $NO_3^- + NO_2^-$ concentration

[12] Nutrient analyses for the cruise transects were carried out at sea by standard colorimetric methods; these data were taken from the CDIAC and JGOFS websites [http://www1.whoi.edu/]. For samples collected during the incubations, water was collected in duplicate at each time point and stored frozen at -20 ° C until subsequent analysis. The sum of [NO_3^- + nitrite (NO_2^-)] (hereafter, [NO_3^-]) was measured by reduction to NO using a solution containing heated, acidic V (III), followed by chemiluminescent detection of NO [*Braman and Hendrix*, 1989]. Standardization was achieved using potassium nitrate. Samples were analyzed in a configuration yielding a limit of detection of 0.03 $\mu mol\ kg^{-1}$ with a precision of $\pm$ 0.025 $\mu mol\ kg^{-1}$ when $[NO_3^-] < 0.1\ \mu mol\ kg^{-1}$ or a limit of detection of 0.1 $\mu mol\ kg^{-1}$ with a precision of 0.05 $\mu mol\ kg^{-1}$ when $[NO_3^-] > 0.1\ \mu mol\ kg^{-1}$.

2.3.4. NH_4^+ concentration

[13] The concentration of NH_4^+ in incubation samples was performed on duplicate samples collected at each time point and measured the same day using a fluorescence technique with orthophthaldialdehyde (OPA) [*Holmes et al*., 1999]. Samples reacted for two hours at room temperature with an OPA-containing solution, with subsequent measurement of fluorescence at an excitation/emission of 350 nm/410-600 nm (Turner Designs Model 7200–000). Standardization was achieved using ammonium chloride. The limit of detection was 0.025 $\mu mol\ kg^{-1}$ with a precision of $\pm$ 0.01 $\mu mol\ kg^{-1}$.

2.3.5. DON concentration

[14] The concentration of DON ([DON]) was calculated by subtracting the sum of dissolved inorganic nitrogen ($[DIN] = [NO_3^- + NO_2^-] + [NH_4^+]$) from the measured [TDN]; [DON] = [TDN] – [DIN]. Propagation of error yields a precision on [DON] measurements of $\pm$ 0.5 $\mu mol\ kg^{-1}$ or a coefficient of variation (CV) of ~10%. Measurements of $[NH_4^+]$ were not performed on the global surface ocean [DON] dataset, as open ocean $[NH_4^+]$ are typically $< 0.1\ \mu mol\ kg^{-1}$ [*Lipschultz*, 2001].

2.3.6. Bacterioplankton cell C

[15] Samples for the enumeration of cell abundance were collected at each time point of the incubation experiments and fixed with particle-free 25% glutaraldehyde (Exp-March) or 10% formalin (Exp-Dec) to a final concentration of 1.0% and stored at 4 ºC until preparation. Cells were filtered onto Irgalan black-stained 0.2-μm polycarbonate filters; samples were stained with 4′–6′-diamidino-2-phenylidole (DAPI) [*Porter and Feig*, 1980] and enumerated with a Nikon Eclipse E400 epifluorescence microscope (1000x). The slope of the regression of cell abundance from the initial time point until the end of the log-phase growth was used to assess whether cell production was significant ($P < 0.05$). Bacterioplankton cell C was calculated from cell abundance using a C conversion factor typical for oceanic bacterial assemblages of 12.4 fg C $cell^{-1}$ [*Fukuda et al*., 1998].

2.4. Statistical Model of Simulated Upper Ocean Tracer Advection

[16] In assessing the timescale of upwelled waters to reach the central gyres, we employed a statistical model of upper ocean tracer advection for waters circulating in the wind-driven Ekman layer (upper 50 m). The simulation is based upon probability distribution functions derived from the trajectories of more than 15,000 satellite-tracked drifting buoys of the Global Drifter Program drogued at 15 meters [*Niiler*, 2001], which reveal the combination of geostrophic and Ekman flow. For each simulation, a tracer is released at a point and integrated forward at one half of one degree resolution for 730 days at 5-day time steps following the description in *Maximenko et al*. [2012] and *Lumpkin et al*. [2012]. The initial release locations were chosen to be the surface waters located at the most equatorward extent of

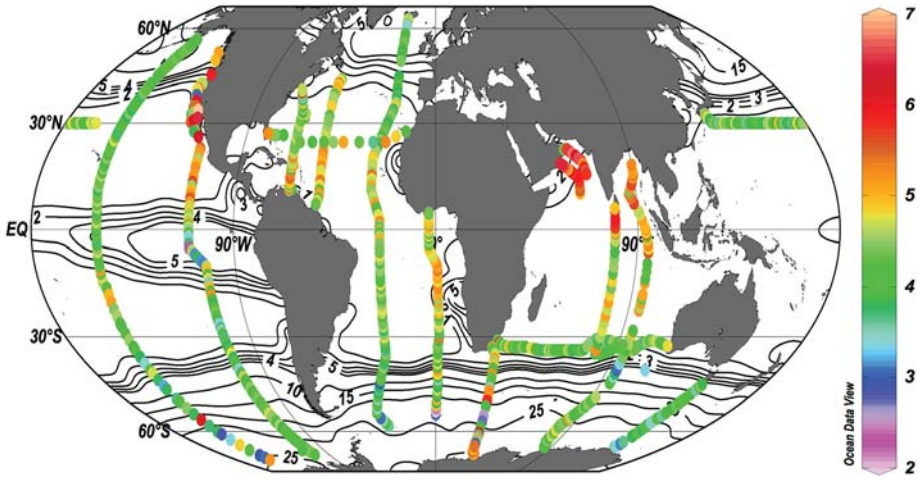

Figure 1. Distribution of [DON] (μmol kg^{-1}; colored dots) at 10 m in the global ocean. Isolines indicate annual mean surface ocean (10 m) [NO_3^-] (μmol kg^{-1}), using gridded data of the World Ocean Atlas, 2005 [http://www.nodc.noaa.gov/]. Atlantic Ocean lines: A13.5 = ~0º E, A16 = ~25º W, A20 = ~52º W, A22 = 66º W, A05 = 24.5º N; Pacific Ocean lines: P18 = ~103º W, P16 = ~150º W, NOAA NACP west coast = ~120ºW, P02 = ~30º N; Indian Ocean lines: I08S-I09N = ~95º E, I08N = ~80º E, I06S = ~30º E, SR03 = ~145º E, I05 = ~34º S, JGOFS Arabian Sea Process Cruise #2 = ~15º N 65º E. Plotting done with Ocean Data View [*Schlitzer*, 2012].

each of the four largest eastern boundary upwelling systems (EBUS), i.e., the northwest African, Benguela, Peru, and western North American upwelling systems.

3. Results

3.1. Surface Ocean DON Distributions

[17] The surface ocean (10 m) distribution of DON is presented in Figure 1. Values ranged from 2 to 7 μmol kg^{-1} (with a mean for all observations of 4.4 ± 0.5 μmol kg^{-1}); however, 75% of all observations fell within the narrow range of 3.8 to 4.8 μmol kg^{-1} (indicated by the green colors in Figure 1). Regions exhibiting [DON] ≥5 μmol kg^{-1} were commonly adjacent to or immediately downstream from eastern boundary and equatorial upwelling zones (as well as the monsoon-driven upwelling system of the Arabian Sea), indicating a source of DON within these systems. Lower DON poleward and westward of these upwelling systems is assumed to reflect a sink for DON within the ocean's subtropical gyres. Concentrations of DON were highly variable within the Southern Ocean due, at least in part, to the large analytical uncertainty in samples containing elevated [NO_3^-] [*Hansell*, 1993]. In general, calculation of DON resulted in a CV >25% at [NO_3^-] >6 μmol kg^{-1}. Where surface [NO_3^-] was <1 μmol kg^{-1}, DON at 10 m plotted against the depth of the top of the nitracline demonstrates an inverse relationship (Figure 2b). The y-axis intercept approaches 4.8 μmol kg^{-1} and corresponds to locations with very shallow nitraclines, whereas DON is ~4.3 μmol kg^{-1} where the nitracline is deepest over the subtropical gyres. A plot of the stock of DON in the upper 50 m versus the depth of the top of the nitracline (Figure 2a) exhibits a similar gradient from ~230 mmol N m^{-2} at locations with shallow nitraclines, decreasing to ~200 mmol N m^{-2} at locations with deep nitraclines over the subtropical gyres.

3.2. Incubation Experiments

3.2.1. Exp-March

3.2.1.1. Surface-Surface

[18] Results for the surface-surface incubations from Exp-March are shown in Figure 3 (red). Both DOC and bacterioplankton cell C were monitored to assure (1) no measurable DOM contamination in our experimental setup and (2) active bacterioplankton growth during the incubations. There was no evidence of contamination by extraneous organic matter; initial DOC within the surface-surface incubation carboys was consistent with mass balance calculations of the DOC resulting from the mixing of surface whole water ([DOC] = 77.7 μmol kg^{-1}) and surface 0.2-μm filtered water ([DOC] = 71.3 μmol kg^{-1}) (data not shown). Bacterioplankton growth was observed, reaching stationary phase after four to seven days and resulting in a ~ten-fold accumulation of cell carbon (Figure 3b). Bacterioplankton growth was supported by a measured consumption of DOC (Figure 3a), showing an average of replicate incubations (± 1 S.D.), ΔDOC = 10.4 ± 0.7 μmol kg^{-1} over the 90-day incubation. TDN averaged (± 1 S.D.) 4.4 ± 0.3 μmol kg^{-1} and remained constant within analytical uncertainty throughout the incubation (Figure 3c), indicating conservation of mass for N within the incubation water. Changes in DON were not observed within the ~0.5 μmol kg^{-1} analytical uncertainty, with the time-course concentration averaging 4.3 ± 0.5 μmol kg^{-1} (Figure 3d). This large uncertainty precludes detection of small changes within the DON pool by measurements of [DON] alone. However, by measuring the products of DON remineralization, NH_4^+ and NO_3^-, which have orders of magnitude lower analytical uncertainty, rates of net DON remineralization can be derived. [NH_4^+] increased to a maximum of ~0.1 μmol kg^{-1} after two weeks, then cycled between ~0.04 and 0.10 μmol kg^{-1} over the remainder of the incubation (Figure 3e). [NO_3^-] was low (≤0.06 μmol kg^{-1}) and

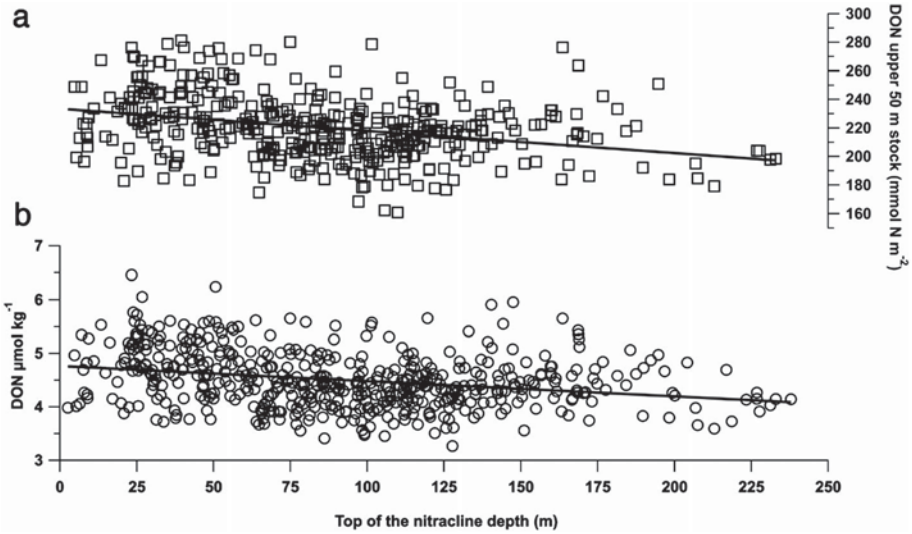

Figure 2. Upper 50 m DON stock (a) (mmol N m^{-2}, open squares) and surface ocean (10 m) [DON] (b) (µmol kg^{-1}; open circles) plotted versus depth (m) of the top of the nitracline (defined as depth where $[NO_3^-] = 1$ µmol kg^{-1}), at all locations where surface $[NO_3^-] < 1$ µmol kg^{-1}. Solid black line is model II reduced major axis regression for (a) [DON stock = (−0.156 x nitracline depth) + 233; $r^2 = 0.10$; n = 405] and (b) [DON = (−0.003 x nitracline depth) + 4.8; $r^2 = 0.07$; n = 516].

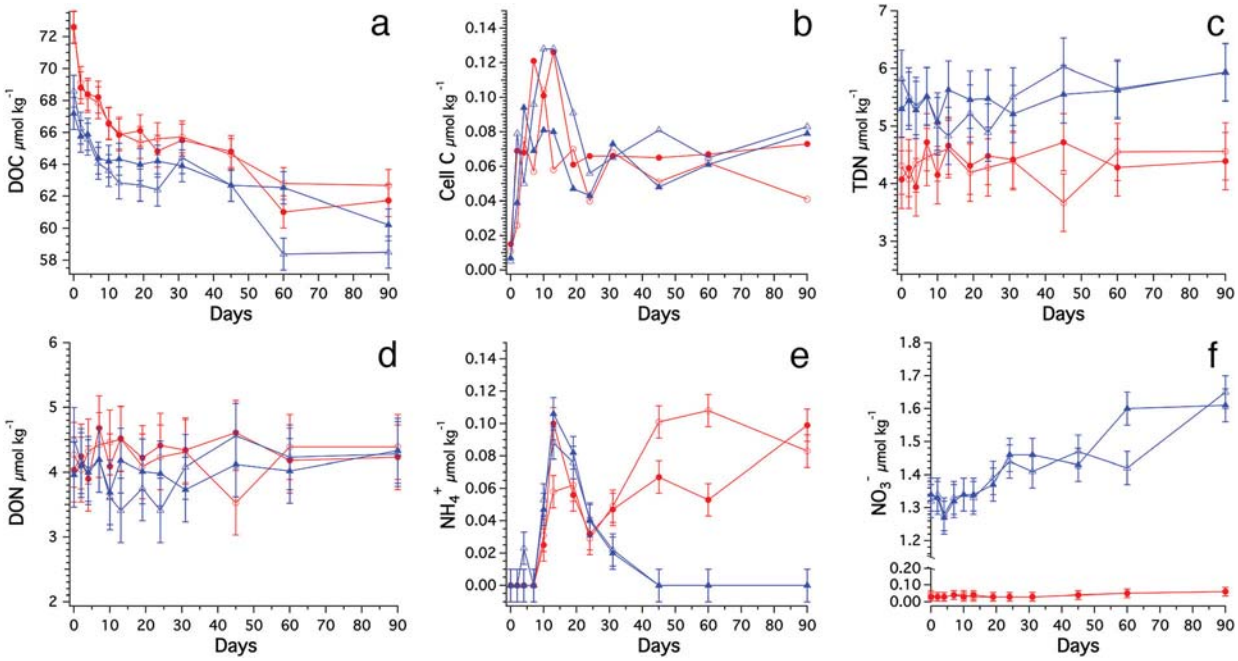

Figure 3. Property time-series for Exp-March: (a) DOC (µmol kg^{-1}), (b) bacterioplankton cell carbon (µmol kg^{-1}), (c) total dissolved nitrogen (TDN, µmol kg^{-1}), (d) DON (µmol kg^{-1}), (e) NH_4^+ (µmol kg^{-1}), and (f) NO_3^- (µmol kg^{-1}). Red colors are surface-surface incubations; open and filled circles represent replicate experiments. Blue colors are surface-meso incubations; open and filled triangles represent replicate experiments. Error bars equal ± 1 S.D.; error bars are omitted from (b) for clarity, SD equals 0.02 µmol C kg^{-1}.

near constant throughout the incubation with no significant increase (ANOVA, $P > 0.10$) (Figure 3f). The production of NH_4^+ indicates that a net of ~0.10 µmol kg^{-1} DON had been mineralized over the course of the incubation.

3.2.1.2. Surface-Meso

[19] Figure 3 shows results from the Exp-March surface-meso incubations (in blue). Initial DOC within the incubation carboys confirmed the absence of measurable contamination and was as expected from mass balance calculations of the predicted DOC resulting from mixing 8 L of surface 0.2-µm filtered water ([DOC] = 71.3 µmol kg^{-1}) and 2 L of mesopelagic water (180 m) ([DOC] = 58.3 µmol kg^{-1}). Bacterioplankton cell C (Figure 3b) and DOC consumption (Figure 3a) were similar in pattern and magnitude to the surface-surface incubation,

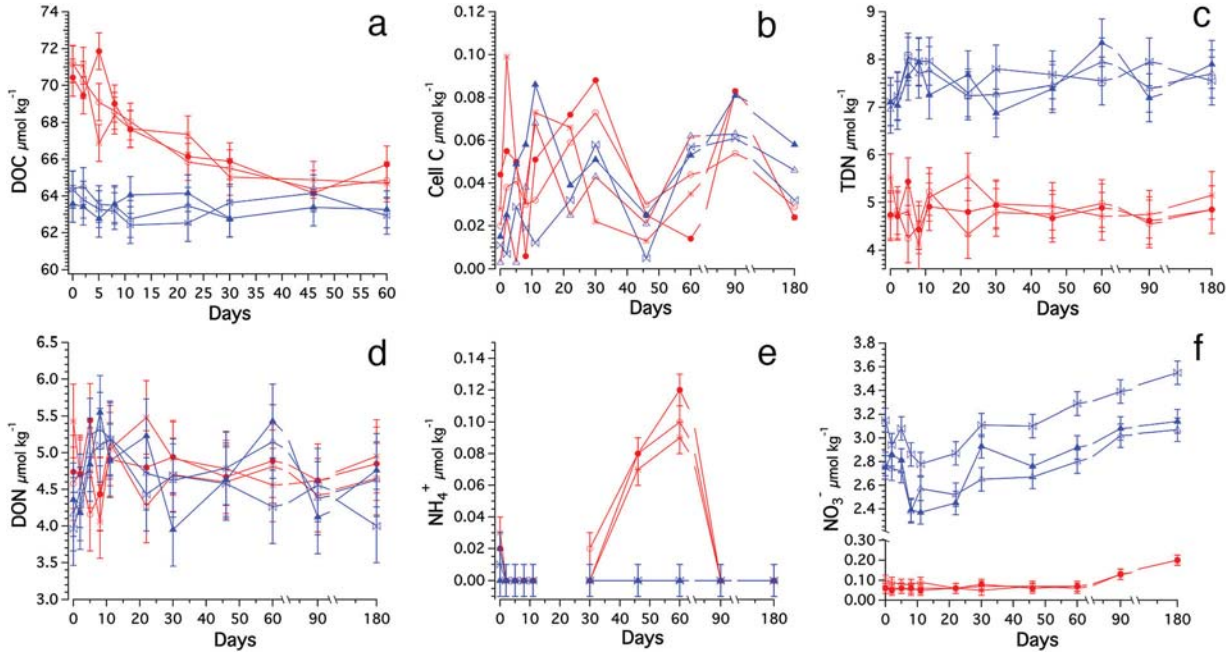

Figure 4. Property time-series for Exp-Dec: (a) DOC (µmol kg^{-1}), (b) bacterioplankton cell carbon (µmol kg^{-1}), (c) total dissolved nitrogen (TDN, µmol kg^{-1}), (d) DON (µmol kg^{-1}), (e) NH_4^+ (µmol kg^{-1}), and (f) NO_3^- (µmol kg^{-1}). Red colors are surface-surface incubations; open/filled circles and stars represent replicate experiments. Blue colors are surface-meso incubations; open/filled triangles and bowties represent replicate experiments. Error bars equal ± 1 S.D.; error bars are omitted from (b) for clarity, S.D. equals ± 0.02 µmol C kg^{-1}.

with a ~ ten-fold accumulation of cell C and net DOC consumption of 8.5 ± 2.2 µmol kg^{-1} after 90 days. Measurements of TDN averaged (± 1 S.D.) 5.4 ± 0.3 µmol kg^{-1} and remained constant (Figure 3c). No changes in DON were observed within the analytical uncertainty, which averaged 4.0 ± 0.5 µmol kg^{-1} (Figure 3d). Similar to the results from the surface-surface incubation, [NH_4^+] increased to ~0.10 µmol kg^{-1} after two weeks (Figure 3e); however, this NH_4^+ was slowly nitrified to NO_3^- over the course of one month, as indicated by the decrease in [NH_4^+] in Figure 3e and an accumulation in [NO_3^-] of 0.30 ± 0.05 µmol kg^{-1} (ANOVA, P <0.0001) over the course of the experiment (Figure 3f). The net accumulation of [NO_3^-] indicated 0.30 ± 0.05 µmol kg^{-1} DON had been consumed by 90 days.

3.2.2. Exp-Dec

3.2.2.1. Surface-Surface

[20] Results for the surface-surface incubations from Exp-Dec are shown in Figure 4 (red). Initial DOC confirmed the absence of contamination during experimental setup (Niskin [DOC] = 75.2 µmol kg^{-1}). DOC was consumed over two months, averaging ΔDOC = 5.8 ± 0.7 µmol kg^{-1} (Figure 4a). Bacterioplankton cell C increased ~ five-fold within the first two weeks of incubation and was variable over the remainder of the experiment (Figure 4b). TDN was constant within analytical uncertainty over the course of the experiment, 4.9 ± 0.5 µmol kg^{-1}, indicating conservation of N mass (Figure 4c). DON averaged (± 1 S.D.) 4.6 ± 0.5 µmol kg^{-1} with no observable change within uncertainty over the 180-day incubation (Figure 4d). [NH_4^+] increased after day 30 to ~0.10 µmol kg^{-1} (Figure 4e), which was then nitrified to NO_3^- as indicated by the [NO_3^-] increase in Figure 4f. The production of NH_4^+ and net accumulation of NO_3^- indicated 0.14 ± 0.05 µmol kg^{-1} (ANOVA, P <0.007) of net DON consumption after 180 days.

3.2.2.2. Surface-Meso

[21] Exp-Dec surface-meso incubation results are shown in Figure 4 (blue). Initial incubation [DOC] was as expected from mass balance calculations of the mixing of 8 L of 0.2-µm filtered surface water ([DOC] = 74.3 µmol kg^{-1}) with 2 L of mesopelagic water from 130 m depth (Niskin [DOC] = 57.4 µmol kg^{-1}), confirming the absence of contamination (Figure 4a). A small net consumption of DOC was observed after ~ two weeks, averaging ΔDOC = 1.4 ± 0.5 µmol kg^{-1} (Figure 4a). Bacterioplankton cell C (Figure 4b) was similar in pattern and magnitude to the Exp-Dec surface-surface incubations (red colors). TDN averaged (± 1 S.D.) 7.5 ± 0.5 µmol kg^{-1} and was constant with time (Figure 4c). No changes were observed within analytical uncertainty for DON, which averaged (± 1 S.D.) 4.6 ± 0.5 µmol kg^{-1} (Figure 4d). [NH_4^+] remained below the detection limit throughout the incubation (Figure 4e). Net accumulation of [NO_3^-] was observed (Figure 4f), averaging (± 1 S.D.) 0.38 ± 0.10 µmol kg^{-1} (ANOVA, P <0.0001), indicating net consumption of DON over 180 days.

3.3. Statistical Model of Simulated Ocean Tracer Advection

3.3.1. Atlantic

[22] The probability density of simulated tracer concentration, in units of log10 (initial concentration), up to one year, is shown for the North and South Atlantic Oceans in

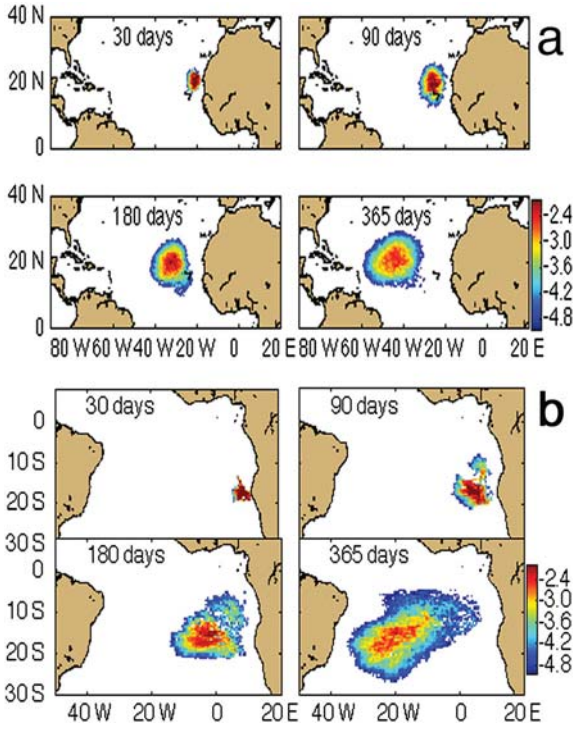

Figure 5. Concentration of simulated tracer after 30, 90, 180, and 365 days since release in (a) the North Atlantic at 21° N 18° W and (b) in the South Atlantic at 18° S 11° E using the statistical model based on surface ocean drifter observations. Color scale is the log10 of concentration where initial concentration is 1.

Figure 5a and Figure 5b, respectively. The penetration of waters exiting the EBUS toward the gyre centers is a slow process, owing to the sluggish surface currents of the eastern limbs of the gyre circulations. After 90 to 180 days, the timescale of our incubation experiments, the core of these waters was located near 20° to 30° west in the North Atlantic. South Atlantic upwelled waters reached ~5° east and 5° west after 90 and 180 days, respectively. Upwelled waters are still within ~1000 km of the coast after six months, only reaching the basin centers after ~1 year.

3.3.2. Pacific

[23] The slow transport toward the subtropical gyres characteristic of the Atlantic Ocean is similar for upwelled waters in the Pacific Ocean. Surface waters leaving the Peru upwelling system travel to ~90° and 100° west after 90 and 180 days, respectively, and reach ~110° west after one year (Figure 6b). Upwelled waters leaving the California current system penetrated even less into the North Pacific gyre, remaining ~500 km from the coast after 90 to 180 days near 120° west, reaching ~130° west after one year (Figure 6a).

4. Discussion

4.1. DON Removal Mechanisms

[24] The surface ocean distribution of DON characterized by enrichment near upwelling regions and depletion of this signal poleward and westward across the subtropical gyres (Figures 1 and 2) implies a sink for DON in the subtropical gyres on the order of ~0.5 μmol kg^{-1} (or ~30 mmol N m^{-2}) from the upper 50 m of the water column (Figure 2). Figure 7 describes potential mechanisms for this DON removal.

[25] In Figure 7a (Mechanism I), DON produced within upwelling zones along the equator or eastern boundary resists immediate utilization and is transported by the surface ocean circulation toward the subtropical gyres. En route, DON is removed by direct assimilation of DON and/or its

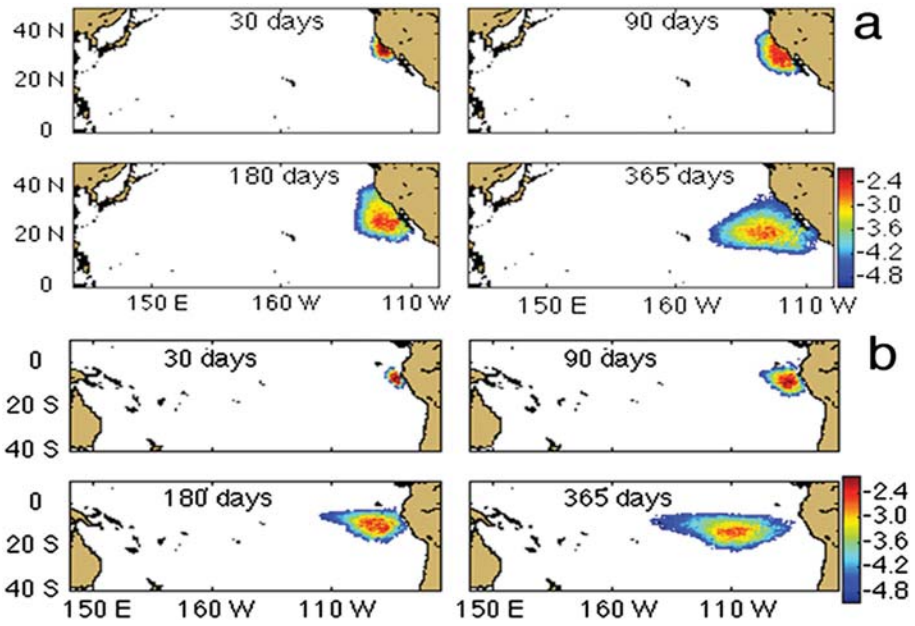

Figure 6. Concentration of simulated tracer after 30, 90, 180, and 365 days since release in the North Pacific at (a) 34° N 121° W (a) and (b) in the South Pacific at 6° S 82° W (b). Color scale is the log10 of concentration where initial concentration is 1.

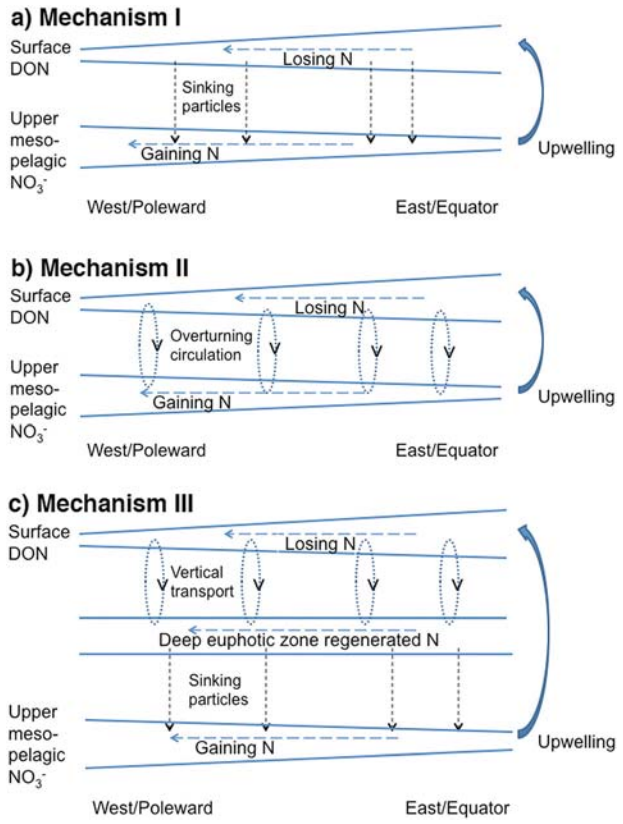

Figure 7. Proposed mechanisms for DON removal from the surface ocean. (a) Mechanism I: Removal via surface consumption of DON and export as sinking particulate N. Oligotrophic gyre export production is directly supported by allochthonous DON input in this model. (b) Mechanism II: Removal of DON upon overturning circulation of the water column to the upper mesopelagic zone where the resident microbial community contains the necessary metabolic capacity to remineralize DON. Gyre export production is not directly supported by allochthonous DON in this model. (c) Mechanism III: Removal via a two-step vertical mixing and sinking particle process. DON is removed from the surface layer via vertical transport to the deep euphotic zone where heterotrophic microbes mineralize DON, regenerating inorganic N for autotrophic production in the deep euphotic zone. This source of new N results in net formation of sinking particles, which remove N from the base of the euphotic zone to the mesopelagic where it is remineralized. This two-step process results in indirect allochthonous DON support of subtropical gyre export production.

remineralization products and supports export production. After sinking out of the euphotic zone, the particulate organic nitrogen is remineralized and accumulates as NO_3^- in the upper mesopelagic zone. Mechanism I is analogous to that proposed by *Roussenov et al.* [2006] and *Torres-Valdés et al.* [2009], and is distinct from the presumed flux of N through the DON pool that supports regenerated production in oligotrophic systems [*Bronk et al.*, 2007; *Knapp et al.*, 2011].

[26] In Mechanism II (Figure 7b), DON removal occurs upon vertical mixing of the upper water column. In this case, DON is largely recalcitrant to utilization by the surface microbial community; instead it is preferentially consumed after being vertically mixed or entrained into the upper mesopelagic water column. This model describes a fate for surface accumulated DON similar to that found for the seasonally accumulated surface ocean DOC pool at the BATS site [*Carlson et al.*, 2004]. Under this mechanism, the lateral input of DON does not have an immediate impact on export production within the subtropical gyres, although it will have an indirect impact in that the NO_3^- produced upon DON remineralization in the mesopelagic is returned to the surface layer with subsequent mixing events.

4.2. Insights From Incubation Experiments

[27] The incubation experiments were designed to examine the lability of surface accumulated DON when exposed to the extant surface microbial assemblages versus mesopelagic microbial assemblages. If the waters investigated from the Florida Straits are representative of the oligotrophic environmental conditions in the adjacent North Atlantic, then the results from these experiments gain insight into the behavior of DON across the ocean's subtropical gyres. The surface-surface incubations tested Mechanism I by evaluating the bioavailability of surface ocean DON to the microbes found there. The surface-meso incubations investigated Mechanism II, testing for microbial utilization of surface ocean DON under conditions simulating overturning circulation.

[28] During the surface-surface incubations, accumulation of NO_3^- and/or NH_4^+ indicated that the maximum quantity of DON mineralized was ~0.1 μmol kg^{-1}. The source of this inorganic N could have been either remineralized particulate organic N (PON, which includes suspended particles and microbial intracellular N) or remineralized DON, as these two pools were not differentiated in our analysis. If, for the purposes of this study, we assume that all of the NH_4^+ produced was by remineralization of DON (initial bulk PON <0.1 μmol kg^{-1} after dilution given surface ocean [PON] = ~0.3 μmol kg^{-1} in the nearby Sargasso Sea [*Hansell and Carlson*, 2001]), then <3% of the surface bulk DON pool was bioavailable to the extant surface ocean microbial community over a period of three to six months. Under natural environmental conditions and natural light fields, both phytoplankton and heterotrophic bacteria would compete for this NH_4^+ [*Kirchman*, 1994], initially supporting regenerated production [*Dugdale and Goering*, 1967]. Assuming steady state for N in the euphotic zone, this N would eventually be exported. The relative recalcitrance of surface ocean DON to microbial utilization within the euphotic zone suggests a limited role for Mechanism I for DON removal within the oligotrophic gyres.

[29] The results of the surface-meso incubations more strongly support a role for Mechanism II in the removal of surface ocean DON from oligotrophic gyres. During Exp-March, the accumulation of 0.30 ± 0.05 μmol kg^{-1} inorganic N throughout the three-month experiment is three times the net remineralization in the surface-surface incubation. During the Exp-Dec surface-meso incubations (Figure 4e), the accumulation of 0.38 ± 0.10 μmol kg^{-1} inorganic N after 180 days (Figure 4f) also indicated a three-fold greater net DON remineralization than observed in the Exp-Dec surface-surface incubations. The potential contribution of PON remineralization to the observed inorganic N accumulation is at most 10% given the likely initial PON on the order of ~0.03 μmol kg^{-1} in the incubation water after dilution

([PON] = ~0.15 μmol kg^{-1} at mesopelagic depths in the Sargasso Sea [*Altabet*, 1988]. Our simulated mixing experiments indicate that DON consumption in the upper mesopelagic occurs on the timescale of months at a rate of ~1 μmol N kg^{-1} yr^{-1}, about three-fold faster than the rate in the surface layer. This upper mesopelagic rate is consistent with both the rate and magnitude of surface ocean DON loss at BATS [*Hansell and Carlson*, 2001; *Knapp et al*., 2005], as well as the Sargasso Sea and North Pacific Gyre [*Knapp et al*., 2011].

4.3. Export of DON-Enriched Waters at the Gyre Margins

[30] Mechanism II requires that two conditions be met: (1) accumulated surface ocean DON is transported to the upper mesopelagic via overturning circulation and (2) it is mineralized there on relatively rapid timescales. The second condition has been demonstrated above, so the first condition must now be tested. Do DON-enriched waters of the EBUS actually mix to subeuphotic zone depths?

[31] We first consider the timescale for transport of surface waters from the upwelling region into the gyre center. If transfer is rapid (i.e., on the order of weeks), then DON-enriched waters may escape subduction at the sites of subtropical mode water formation at the eastern gyre margins, thus being retained in the upper 50 m within the central subtropical gyres. By contrast, if transfer is slow, DON-enriched waters may persist at the gyre margins long enough to be mixed vertically prior to significant horizontal penetration into the gyre center.

[32] The relatively slow transport of upwelled waters toward the gyre centers observed in both the North and South Atlantic (Figure 5) indicates that the DON-enriched surface waters of EBUS are mixed vertically and/or subducted during wintertime convective mixing prior to transport into the gyre center. If we assume upwelled waters leaving the NW African and Benguela EBUS begin transit toward the gyre in the summer months [*Chavez and Messié*, 2009], six months later (in midwinter) the core of these waters reach ~30º W in the North Atlantic (Figure 5a) and ~5º W in the South Atlantic (Figure 5b), respectively.

[33] During winter mixing, surface water density reaches maximum values, and DON will be subducted to the corresponding isopycnal surface. For the northeast subtropical Atlantic, wintertime (January-March) convective mixing reaches a maximum surface density of sigma-theta 24.0 to 26.0 (Figure 8a), thus redistributing the DON-enriched surface waters into this density range. In the summer months (July-September), the water column is capped by a lighter density layer of sigma-theta 23.0 to 25.0 (Figure 8b), causing the subducted, DON-enriched waters to penetrate the gyre along the sigma-theta 25.0 to 26.0 density horizon. Similar seasonal mixing dynamics in the South Atlantic result in the DON-enriched waters leaving the Benguela upwelling system to be subducted within essentially the same density horizon of sigma-theta 25.0 to 26.0 (Figures 8a and 8b).

[34] The exported DON leaves the euphotic zone and enters the upper mesopelagic to the extent that this isopycnal layer does so. The sigma-theta 25.0 to 26.0 surface reaches a maximum depth of ~100 m in the eastern basins in winter (Figures 8c and 8d). This relatively shallow mixing retains DON-enriched waters within the euphotic zone (typical euphotic zone depths are ~100 to 130 m in the eastern sectors of the gyres where subduction occurs [http://disc.sci.gsfc.nasa.gov/giovanni/]). In fact, the farther west the surface waters reach before the onset of overturning circulation, the lighter the density surface these waters would subduct to (Figures 8a and 8b); thus the DON-enriched water would be retained at shallower depths (i.e., ~50 to 100 m). These physical dynamics may preclude subducted DON from escaping the euphotic zone within the eastern sectors of the subtropical gyre.

[35] Surface waters that subduct in the eastern subtropical Pacific Ocean reach a maximum density of sigma-theta 25.0 in both the North and South Pacific (Figures 9a and 9b, respectively). These waters are capped in the summer months by the surface layer with a density of sigma-theta ~24.0 (Figures 9a and 9b). Again assuming that upwelled waters begin their transit toward the gyre during the summer months [*Chavez and Messié*, 2009], six months later (midwinter) the core of these waters reach ~120º W in the North Pacific (Figure 6a) and ~90º W in the South Pacific (Figure 6b). In these regions, subducted water in the sigma-theta 24.0 to 25.0 layer penetrates to a maximum depth of ~100 m with wintertime mixing (Figures 9c and 9d). Shallow vertical mixing prevents DON from penetrating below the euphotic zone in the eastern Pacific basins, similar to the physical constraints in the Atlantic.

[36] It appears that the first condition required for Mechanism II is not observed; DON-enriched waters of the EBUS do not actually mix to subeuphotic zone depths.

4.4. The Fate of DON Within Ocean Subtropical Gyres and Related Uncertainties

[37] It appears that subduction of surface water enriched in DON in the eastern sector of each ocean basin, and its presumed removal at depth, contributes to the observed [DON] zonal gradient at the surface (as described by Mechanism II; Figure 7b), but that export of DON is relatively shallow (i.e., to the deep euphotic zone). The relative recalcitrance of DON to surface microbial communities and its three-fold greater bioavailability to mesopelagic microbes (Figures 3 and 4) is consistent with Mechanism II. These findings limit the role for allochthonous DON to directly support export production across ocean subtropical gyres (as required in Mechanism I; Figure 7a). However, overturning circulation in the eastern basins appears to be restricted to depths shallower than 100 m, thus retaining the DON-enriched waters within the euphotic zone.

[38] If subsequent mineralization of the subducted DON primarily occurs within the deep euphotic zone (~50 to 100 m), any additional export production supported by remineralized DON must occur via a two-step process (Mechanism III; Figure 7c). In this model, DON is exported to the deep euphotic zone with winter mixing, where it is rapidly mineralized. This mechanism requires that a microbial assemblage capable of remineralizing DON at rates similar to the microbes we tested in the upper mesopelagic (~130 to 180 m) is active at the base of the euphotic zone. While some vertical overlap in microbial assemblages occurs in the upper ~500 m, vertically stratified bacterial communities are typically partitioned according to physical and chemical gradients [*Morris et al*., 2005; *Carlson et al*., 2009; *Treusch et al*., 2009]. For example, the microbial community within

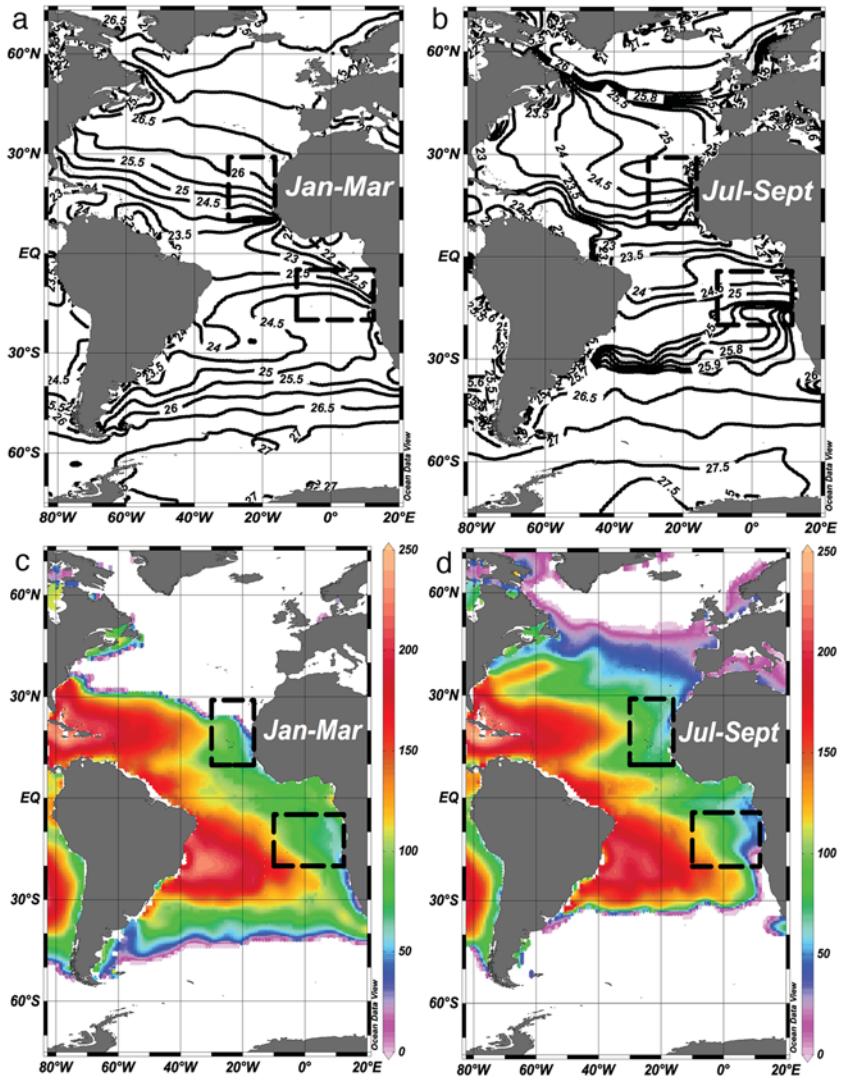

Figure 8. Mean geographic distribution of surface outcrops of isopycnal surfaces in the Atlantic for (a) January–March and (b) July–September. Depths of the sigma-theta 26.0 isopycnal surface for (c) January–March and (d) July–September. Black dashed boxes indicate the regions of transit for waters from the eastern boundary upwelling systems towards the gyre centers within 6 months of upwelling (determined from drifter observations in Figure 5). Plots created using data from the World Ocean Atlas, 2005 [http://www.nodc.noaa.gov/].

the DCM (~120 m depth) at the BATS site was distinct from that in the upper mesopelagic (200 to 300 m) [*Treusch et al*., 2009]; thus it is unclear whether DCM microbial communities harbor similar capabilities for mineralization of surface accumulated DON. In support of Mechanism III, *Knapp et al*. [2011] observed a statistically significant decrease in [DON] of ~0.5 µM below the mixed layer, i.e., within the DCM (~60 to 100 m) of the Sargasso Sea, with a further ~0.5 µM [DON] decrease in the upper mesopelagic (100–200 m) zone.

[39] These results suggest that the primary fate of surface DON is removal via vertical mixing and subsequent mineralization below the mixed layer (<50 m). DON may contribute to export production near the eastern edges of the subtropical gyres via an indirect two-step process (Mechanism III); however, investigation of the DON mineralization potential of DCM microbial communities is required to validate the model.

[40] One further uncertainty is that the primary DON removal mechanism considered here, remineralization by heterotrophic bacterioplankton, may not be the only process removing DON in surface ocean waters. While photo-mineralization of DON to inorganic species such as NH_4^+ and NO_2^- occurs with exposure to UV light in near surface waters [*Bushaw et al*., 1996; *Kieber et al*., 1999; *Vähätalo and Zepp*, 2005; *Stedmon et al*., 2007], these studies have focused on dissolved humics and terrigenous DOM within coastal regions. The photo-oxidation of marine-produced organic matter is not well constrained in the open ocean. Phytoplankton are also capable of utilizing low molecular weight DON moieties such as urea [*Bronk et al*., 2007], providing a third potential sink for surface accumulated DON. However, much of the DON found in

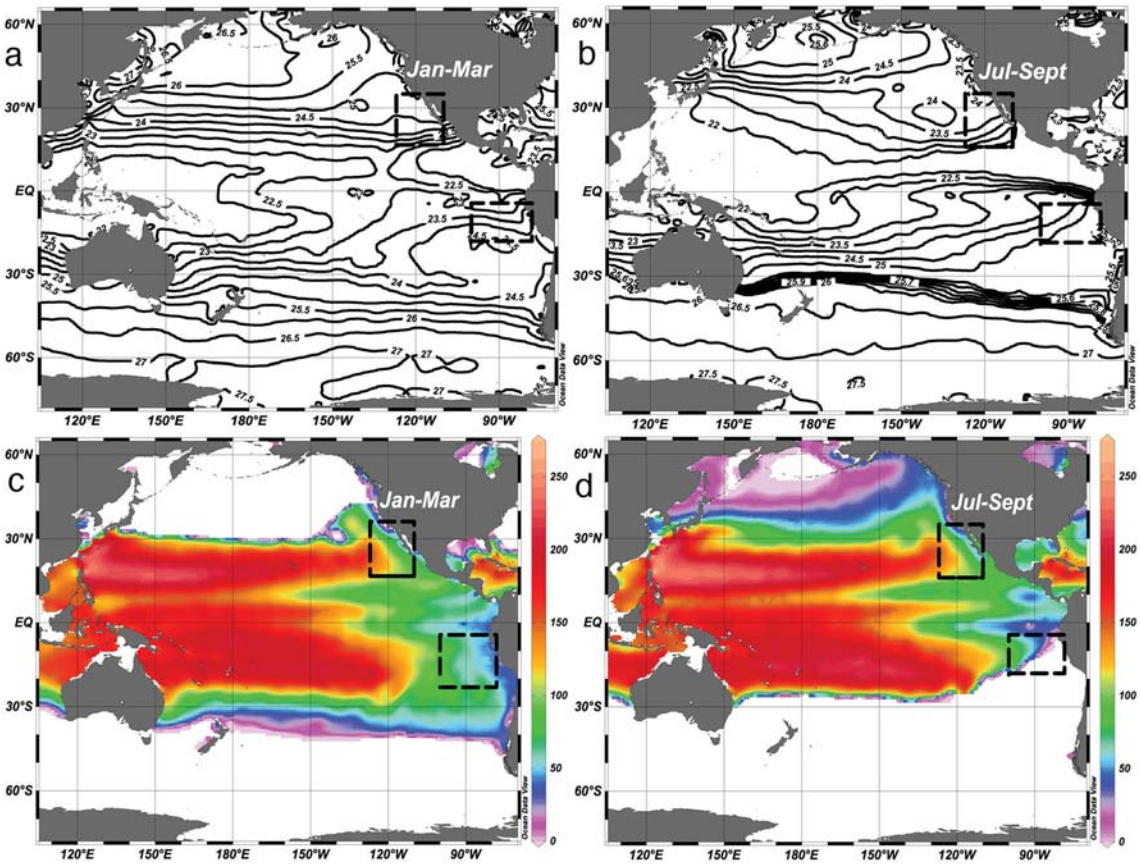

Figure 9. Mean geographic distribution of surface outcrops of isopycnal surfaces in the Pacific for (a) January–March and (b) July–September. Depths of the sigma-theta 25.0 isopycnal for (c) January–March and (d) July–September. Black dashed boxes indicate the regions of transit for waters from the eastern boundary upwelling system towards the gyre centers within 6 months of upwelling (determined from drifter observations in Figure 6). Plots created using data from the World Ocean Atlas, 2005 [http://www.nodc.noaa.gov/].

open ocean surface waters occurs as larger, complex organic molecules with amide functional groups [*McCarthy et al*., 1997; *Aluwihare et al*., 2005] that are thought to be largely unavailable to photoautotrophs, instead requiring extracellular breakdown by microbes to release N [*Berges and Mulholland*, 2008]. Thus, alternative surface ocean sinks for DON not tested in our incubation experiments are considered unlikely to contribute significantly to DON removal in the euphotic zone.

5. Concluding Remarks

[41] We presented the global surface ocean DON distribution and observed a global mean concentration of 4.4 ± 0.5 μmol kg^{-1} within the upper 50 meters. Elevated [DON] (≥5 μmol kg^{-1}) was found in waters adjacent to and downstream from the major upwelling zones. Zonal gradients in surface ocean [DON] indicate a sink of this material within the gyres on the order of ~0.5 μmol kg^{-1} (~30 mmol N m^{-2}) from the upper 50 m, and we explored two possible mechanisms for this DON loss: removal by autotrophic utilization with export of sinking particulate N from the euphotic zone (Mechanism I) or by vertical transport to the mesopelagic zone with subsequent consumption (Mechanism II). Incubation experiments designed to test the biological capacity for surface ocean DON removal found DON to be mostly recalcitrant to utilization by surface ocean microbes; instead DON remineralization occurred with exposure to the heterotrophic microbial community from the upper mesopelagic zone at a rate of ~1 μmol N kg^{-1} yr^{-1}. These results suggest a limited role for DON removal via Mechanism I.

[42] The estimated time scale for transport of DON-enriched waters from the upwelling zones to the interior of the subtropical gyres was found to be long (months to years), allowing the excess DON to persist at the gyre margins long enough to be subducted upon wintertime convection, thus supporting Mechanism II. However, the depth of subduction was shallow (<100 m), so DON and its products would be retained within the deep euphotic zone. If relatively fast remineralization of DON occurs there, this new N could support phytoplankton growth and particle export from the DCM, described as a two-step process (Mechanism III).

[43] We conclude that the primary fate for surface DON is removal via vertical transport to and subsequent mineralization below the mixed layer. The precise depth at which the DON is mineralized (i.e., within or below the deep euphotic zone) determines the potential importance for DON to support export production in the subtropical gyres (i.e., Mechanism II versus III). If the euphotic zone is sufficiently deep, Mechanism III may operate in the eastern sectors of the major ocean basins,

thus providing indirect support of export production after mineralization of DON to NO_3^- within the deep euphotic zone. We found little support for a direct role for allochthonous DON to sustain export production from the mixed layer in the interior of oligotrophic gyres (Mechanism I). Future work should explicitly test Mechanism III by investigating the DON mineralization potential of DCM microbial assemblages. Additionally, quantification of the photo-oxidative DON sink in the open ocean is necessary.

[44] **Acknowledgments.** The authors received support for this work from the National Science Foundation: grant NSF OCE-0752972 to DAH and CAC for the U.S. Global Ocean Carbon and Repeat Hydrography Program; and grant NSF OCE-0933076 to ANK. RL acknowledges support from NOAA's Climate Program Office and the Atlantic Oceanographic and Meteorological Laboratory. We wish to thank all the P.I.'s, crew, and scientists involved with US Global Ocean Carbon and Repeat Hydrography program; their tireless efforts have made this study possible. Wenhao Chen and Charles Farmer (RSMAS) and Elisa Halewood and Maverick Carey (UCSB) are thanked for DOC and TDN analyses. Dr. Chris Sinigalliano (NOAA/AOML) is thanked for help and use of his equipment for DAPI counts.

References

Abell, J., S. Emerson, and P. Renaud (2000), Distributions of TOP, TON and TOC in the North Pacific subtropical gyre: Implications for nutrient supply in the surface ocean and remineralization in the upper thermocline, *J. Mar. Res.*, *58*(2), 203–222.

Altabet, M. A. (1988), Variations in nitrogen isotopic composition between sinking and suspended particles: implications for nitrogen cycling and particle transformation in the open ocean, *Deep Sea Res.*, *35*(4), 535–554.

Aluwihare, L. I., and T. Meador (2008), *Chemical composition of marine dissolved organic nitrogen, in Nitrogen in Marine Environment*, 2nd ed., edited by D. G. Capone et al., pp. 1–50, Academic Press, Burlington, MA, doi:10.1016/B978-0-12-372522-6.00003-7.

Aluwihare, L. I., D. J. Repeta, S. Pantoja, and C. G. Johnson (2005), Two chemically distinct pools of organic nitrogen accumulate in the ocean, *Science*, *308*(5724), 1007–1010, doi:10.1126/science.1108925.

Amon, R. M. W., and R. Benner (1996), Bacterial utilization of different size classes of dissolved organic matter, *Limnol. Oceanogr.*, *41*(1), 41–51.

Berges, J. A., and M. R. Mulholland. (2008), Enzymes and nitrogen cycling, in *Nitrogen in Marine Environment*, 2nd ed., edited by D. G. Capone et al., pp. 1385–1444, Academic Press, Burlington, MA, doi:10.1016/B978-0-12-372522-6.00032-3.

Braman, R. S., and S. A. Hendrix (1989), Nanogram nitrite and nitrate determination in environmental and biological materials by vanadium(III) reduction with chemiluminescence detection, *Anal. Chem.*, *61*(24), 2715–2718.

Bronk, D. A. (2002), Dynamics of DON, in *Biogeochemistry of Marine Dissolved Organic Matter*, 1st ed., edited by D. A. Hansell and C. A. Carlson, pp. 153–247, Academic Press, San Diego, CA, doi:10.1016/B978-012323841-2/50007-5.

Bronk, D. A., J. H. See, P. Bradley, and L. Killberg (2007), DON as a source of bioavailable nitrogen for phytoplankton, *Biogeosciences*, *4*(3), 283–296, doi:10.5194/bg-4-283-2007.

Bushaw, K. L., R. G. Zepp, M. A. Tarr, D. Schulz-Jander, R. A. Bourbonniere, R. E. Hodson, W. L. Miller, D. A. Bronk, and M. A. Moran (1996), Photochemical release of biologically available nitrogen from aquatic dissolved organic matter, *Nature*, *381*(6581), 404–407.

Carlson, C. A., R. Morris, R. Parsons, A. H. Treusch, S. J. Giovannoni, and K. Vergin (2009), Seasonal dynamics of SAR11 populations in the euphotic and mesopelagic zones of the northwestern Sargasso Sea, *ISME J.*, *3*(3), 283–295, doi:10.1038/ismej.2008.117.

Carlson, C. A., S. J. Giovannoni, D. A. Hansell, S. J. Goldberg, R. Parsons, and K. Vergin (2004), Interactions among dissolved organic carbon, microbial processes, and community structure in the mesopelagic zone of the northwestern Sargasso Sea, *Limnol. Oceanogr.*, *49*(4 I), 1073–1083, doi:10.4319/lo.2004.49.4.1073.

Charria, G., I. Dadou, J. Llido, M. Drévillon, and V. Garçon (2008), Importance of dissolved organic nitrogen in the north Atlantic Ocean in sustaining primary production: A 3-D modelling approach, *Biogeosciences*, *5*(5), 1437–1455, doi:10.5194/bg-5-1437-2008.

Chavez, F. P., and M. Messié (2009), A comparison of Eastern Boundary Upwelling Ecosystems, *Prog. Oceanogr.*, *83*(1–4), 80–96, doi:10.1016/j.pocean.2009.07.032.

Cullen, J. J., and R. W. Eppley (1981), Chlorophyll maximum layers of the southern California Bight and possible mechanisms of their formation and maintenance, *Oceanol. Acta*, *4*, 23–32.

Dugdale, R. C., and J. J. Goering (1967), Uptake of new and regenerated forms of nitrogen in primary productivity, *Limnol. Oceanogr.*, *12*(2), 196–206.

Dickson, A.G., C.L. Sabine, and J.R. Christian (Eds.) (2007) Guide to best practices for ocean CO_2 measurements, PICES Special Publication 3, 191.

Fukuda, R., H. Ogawa, T. Nagata, and I. Koike (1998), Direct determination of carbon and nitrogen contents of natural bacterial assemblages in marine environments, *Appl. Environ. Microb.*, *64*(9), 3352–3358.

Gruber, N., and J. L. Sarmiento (1997), Global patterns of marine nitrogen fixation and denitrification, *Global. Biogeochem. Cy.*, *11*(2), 235–266.

Hansell, D. A. (1993), Results and observations from the measurement of DOC and DON in seawater using a high-temperature catalytic oxidation technique, *Mar. Chem.*, *41*(1–3), 195–202.

Hansell, D.A. (2005), Dissolved organic carbon reference material program, *EOS Transactions AGU*, *86*(35), 318, doi:10.1029/2005EO350003.

Hansell, D. A., and C. A. Carlson (2001), Biogeochemistry of total organic carbon and nitrogen in the Sargasso Sea: Control by convective overturn, *Deep Sea Res. Pt. II*, *48*(8–9), 1649–1667.

Hansell, D. A., and T. Y. Waterhouse (1997), Controls on the distributions of organic carbon and nitrogen in the eastern Pacific Ocean, *Deep Sea Res. Part I: Oceanogr. Res. Pap.*, *44*(5), 843–757.

Hansell, D. A., N. R. Bates, and D. B. Olson (2004), Excess nitrate and nitrogen fixation in the North Atlantic Ocean, *Mar. Chem.*, *84*(3–4), 243–265, doi:10.1016/j.marchem.2003.08.004.

Hautala, S. L., and D. H. Roemmich (1998), Subtropical mode water in the Northeast Pacific Basin, *J. Geophys. Res. C: Oceans*, *103*(3336), 13055–13066.

Holmes, R. M., A. Aminot, R. Kérouel, B. A. Hooker, and B. J. Peterson (1999), A simple and precise method for measuring ammonium in marine and freshwater ecosystems, *Can. J. Fish. Aquat. Sci.*, *56*(10), 1801–1808.

Jenkins, W. J., and D. W. R. Wallace (1992), Tracer based inferences of new primary production in the sea, in *Primary Productivity and Biogeochemical Cycles in the Sea*, issue 37, edited by P. G. Falkowski and A. D. Woodhead, pp. 299–314, Springer, New York.

Kieber, R. J., A. Li, and P. J. Seaton (1999), Production of nitrite from the photodegradation of dissolved organic matter in natural waters, *Envir. Sci. Tech.*, *33*(7), 993–998.

Kirchman, D. L. (1994), The uptake of inorganic nutrients by heterotrophic bacteria, *Microb. Ecol.*, *28*(2), 255–271.

Knapp, A. N., D. M. Sigman, and F. Lipschultz (2005), N isotopic composition of dissolved organic nitrogen and nitrate at the Bermuda Atlantic Time-series study site, *Global. Biogeochem. Cy.*, *19*(1), 1–15, doi:10.1029/2004GB002320.

Knapp, A. N., D. M. Sigman, F. Lipschultz, A. B. Kustka, and D. G. Capone (2011), Interbasin isotopic correspondence between upper-ocean bulk DON and subsurface nitrate and its implications for marine nitrogen cycling, *Global. Biogeochem. Cy.*, *25*(4), doi:10.1029/2010GB003878.

Lipschultz, F. (2001), A time-series assessment of the nitrogen cycle at BATS, *Deep Sea Res. Pt. II*, *48*(8–9), 1897–1924.

Lumpkin, R., N. Maximenko, and M. Pazos (2012), Evaluating where and why drifters die, *J. Atmos. Ocean. Tech.*, *29*(2), 300–308, doi:10.1175/JTECH-D-11-00100.1.

Mahaffey, C., R. G. Williams, G. A. Wolff, and W. T. Anderson (2004), Physical supply of nitrogen to phytoplankton in the Atlantic Ocean, *Global. Biogeochem. Cy.*, *18*(1), GB1034, 1–12.

Maximenko, N., J. Hafner, and P. Niiler (2012), Pathways of marine debris derived from trajectories of Lagrangian drifters, *Mar. Pollut. Bull.*, *65*(1–3), 51–62, doi:10.1016/j.marpolbul.2011.04.016.

McCarthy, M., T. Pratum, J. Hedges, and R. Benner (1997), Chemical composition of dissolved organic nitrogen in the ocean, *Nature*, *390*(6656), 150–154.

McCarthy, M. D., R. Benner, C. Lee, J. I. Hedges, and M. L. Fogel (2004), Amino acid carbon isotopic fractionation patterns in oceanic dissolved organic matter: An unaltered photoautotrophic source for dissolved organic nitrogen in the ocean? *Mar. Chem.*, *92*(1–4), 123–134, doi:10.1016/j.marchem.2004.06.021.

Morris, R. M., K. L. Vergin, J. Cho, M. S. Rappé, C. A. Carlson, and S. J. Giovannoni (2005), Temporal and spatial response of bacterioplankton lineages to annual convective overturn at the Bermuda Atlantic Time-series Study site, *Limnol. Oceanogr.*, *50*(5), 1687–1696, doi:10.4319/lo.2005.50.5.1687.

Niiler, P. P. (2001), The world ocean surface circulation, in *Ocean Circulation and Climate*, International Geophysics Series, Vol. *77*, edited by G. Siedler et al., pp. 193–204, Academic Press, New York.

Palenik, B., and F. M. M. Morel (1991), Amine oxidases of marine phytoplankton, *Appl. Environ. Microb.*, *57*(8), 2440–2443.

Porter, K. G., and Y. S. Feig (1980), The use of DAPI for identifying and counting aquatic microflora, *Limnol. Oceanogr. 25*, 943–948.

Roussenov, V., R. G. Williams, C. Mahaffey, and G. A. Wolff (2006), Does the transport of dissolved organic nutrients affect export production in the Atlantic Ocean? *Global. Biogeochem. Cy.*, *20*(3), doi:10.1029/2005GB002510.

Schlitzer, R. (2012), Ocean Data View 4, http://odv.awi.de

Siedler, G., A. Kuhl, and W. Zenk (1987), The Madeira mode water, *J. Phys. Oceanogr.*, *17*, 1561–1570, doi:10.1175/1520-0485(1987)017<1561:TMMW>2.0.CO;2.

Stedmon, C. A., S. Markager, L. Tranvik, L. Kronberg, T. Slätis, and W. Martinsen (2007), Photochemical production of ammonium and transformation of dissolved organic matter in the Baltic Sea, *Mar. Chem.*, *104* (3–4), 227–240, doi:10.1016/j.marchem.2006.11.005.

Torres-Valdés, S., V. M. Roussenov, R. Sanders, S. Reynolds, X. Pan, R. Mather, A. Landolfi, G. A. Wolff, E. P. Achterberg, and R. G. Williams (2009), Distribution of dissolved organic nutrients and their effect on export production over the Atlantic Ocean, *Global. Biogeochem. Cy.*, *23*(4), doi:10.1029/2008GB003389.

Treusch, A. H., K. L. Vergin, L. A. Finlay, M. G. Donatz, R. M. Burton, C. A. Carlson, and S. J. Giovannoni (2009), Seasonality and vertical structure of microbial communities in an ocean gyre, *ISME J.*, *3*(10), 1148–1163, doi:10.1038/ismej.2009.60.

Vähätalo, A. V., and R. G. Zepp (2005), Photochemical mineralization of dissolved organic nitrogen to ammonium in the Baltic Sea, *Envir. Sci. Tech.*, *39*(18), 6985–6992, doi:10.1021/es050142z.

Walsh, T. W. (1989), Total dissolved nitrogen in seawater: a new high temperature combustion method and a comparison with photo-oxidation, *Mar. Chem.*, *26*(4), 295–311.

Ward, B. B., K. A. Kilpatrick, E. H. Renger, and R. W. Eppley (1989), Biological nitrogen cycling in the nitracline, *Limnol. Oceanogr.*, *34(3)*, 493–513.

Williams, R. G., and M. J. Follows (1998), The Ekman transfer of nutrients and maintenance of new production over the North Atlantic, *Deep Sea Res. Part I: Oceanogr. Res. Pap.*, *45*(2–3), 461–489.